Langmuir
Article
pubs.acs.org/Langmuir
© 2009 American Chemical Society

# Solubilized Derivatives of Perylenetetracarboxylic Dianhydride (PTCDA) Adsorbed on Highly Oriented Pyrolytic Graphite

James C. Russell,[†] Matthew O. Blunt,[†] Gudrun Goretzki,[‡] Anna G. Phillips,[‡] Neil R. Champness,[‡] and Peter H. Beton*,[†]

[†]*School of Physics and Astronomy, University of Nottingham, University Park, Nottingham, U.K., and* [‡]*School of Chemistry, University of Nottingham, University Park, Nottingham, U.K.*

*Received September 4, 2009. Revised Manuscript Received November 20, 2009*

The effect on 2D molecular crystallization caused by the addition of propylthioether side groups to the 3,4,9,10-perylenetetracarboxylic dianhydride (PTCDA) molecule is investigated using scanning tunneling microscopy (STM). The molecule was deposited from 1-phenyloctane onto highly oriented pyrolytic graphite (HOPG) and imaged at the liquid−solid interface. We observe a different structure to previously reported arrangements of PTCDA due to the presence of the propylthioether side groups which inhibits the formation of the herringbone phase. A model, supported by calculations based on density functional theory, is proposed in which molecules form rows stabilized by hydrogen bonding.

## Introduction

The molecule perylenetetracarboxylic dianhydride, PTCDA, has been widely studied as a prototype active material for organic electronic devices.[1,2] PTCDA may be readily deposited by vacuum deposition, and the properties of the resulting thin films have been investigated on a variety of different substrates including HOPG,[3,4] Ag(111),[5] Au(111),[6] Ag/Si(111)-($\sqrt{3} \times \sqrt{3}$),[7−9] Sn/Si(111)-($2\sqrt{3} \times \sqrt{3}$),[10] and Cu(111).[11] In recent studies the interest in sublimed monolayers of PTCDA has been extended through the demonstration of the covalent coupling of adsorbed PTCDA to a variety of amine compounds,[12,13] leading to the identification of two-dimensional disordered polymers. This process is closely related to a reaction that occurs in solution phase where the substitution of the anhydride group with an alkane chain attached via an imide group leads to a family of compounds which have been widely investigated.[14−17]

The addition of an imide-linked alkane chain promotes solubility of the resulting molecule, but the anhydride group of the PTCDA is eliminated through this coupling. In fact, and despite the extensive literature describing the adsorption of PTCDA under vacuum conditions, there have been very few studies of solution deposition of PTCDA due to its limited solubility.[18] Nevertheless, the controlled adsorption of arrays of molecules onto surfaces from a solution phase has become increasingly relevant to the fields of nanoscience and nanotechnology for the purposes of fabricating small electronic devices and sensors.[19,20]

In this paper, we investigate a possible route to solubilizing PTCDA which leaves intact the anhydride functionality and show that such a modified derivative may be deposited on a substrate from a solution phase. The solubility is promoted by the introduction of a propyl chain attached to each side of the PTCDA molecule via a thioether link. The di(propylthio)perylenetetracarboxylic dianhydride (DPT-PTCDA) molecule is shown in Figure 1.

## Experimental Section

The DPT-PTCDA molecules were synthesized using the same procedure as summarized in previous work.[21] The molecules were dissolved in 1-phenyloctane (Sigma-Aldrich, 97% purity). A 10 $\mu$L droplet of solution was removed using a pipet and deposited onto a freshly cleaved HOPG surface. An Agilent 4500 series SPM was used to perform the imaging experiments in conjunction with the PicoScan control box and software. The STM was mounted in an isolation chamber with acoustic and vibrational damping to reduce environmental effects. Fresh STM tips were mechanically cut from 0.25 mm (80:20) PtIr wire before each experiment. The quality of the mechanically cut tips was

*Corresponding author. E-mail: peter.beton@nottingham.ac.uk.

(1) Forrest, S. R. *Chem. Rev.* **1997**, *97*, 1793–1896.
(2) Schreiber, F. *Phys. Status Solidi A* **2004**, *201*, 1037–1054.
(3) Hoshino, A.; Isoda, S.; Kurata, H.; Kobayashi, T. *J. Appl. Phys.* **1994**, *76*, 4113–4120.
(4) Kendrick, C.; Kahn, A.; Forrest, S. R. *Appl. Surf. Sci.* **1996**, *104*, 586–594.
(5) Glocker, K.; Seidel, C.; Soukopp, A.; Sokolowski, M.; Umbach, E.; Bohringer, M.; Berndt, R.; Schneider, W. D. *Surf. Sci.* **1998**, *405*, 1–20.
(6) Chizhov, I.; Kahn, A.; Scoles, G. *J. Cryst. Growth* **2000**, *208*, 449–458.
(7) Gustafsson, J. B.; Zhang, H. M.; Johansson, L. S. O. *Phys. Rev. B* **2007**, *75*, 155414.
(8) Ma, J.; Rogers, B. L.; Humphry, M. J.; Ring, D. J.; Goretzki, G.; Champness, N. R.; Beton, P. H. *J. Phys. Chem. B* **2006**, *110*, 12207–12210.
(9) Swarbrick, J. C.; Ma, J.; Theobald, J. A.; Oxtoby, N. S.; O'Shea, J. N.; Champness, N. R.; Beton, P. H. *J. Phys. Chem. B* **2005**, *109*, 12167–12174.
(10) Nicoara, N.; Wei, Z.; Gomez-Rodriguez, J. M. *J. Phys. Chem. C* **2009**, *113*, 14935−40.
(11) Wagner, T.; Bannani, A.; Bobisch, C.; Karacuban, H.; Moller, R. *J. Phys.: Condens. Matter* **2007**, *19*, 056009.
(12) Treier, M.; Richardson, N. V.; Fasel, R. *J. Am. Chem. Soc.* **2008**, *130*, 14054–14055. Treier, M.; Nguyen, M.-T.; Richardson, N. V.; Pignedoli, C.; Passerone, D.; Fasel, R. *Nano Lett.* **2009**, *9*, 126–131.
(13) Treier, M.; Fasel, R.; Champness, N. R.; Argent, S.; Richardson, N. V. *Phys. Chem. Chem. Phys.* **2009**, *11*, 1209–1214.
(14) Briseno, A. L.; Mannsfeld, S. C. B.; Reese, C.; Hancock, J. M.; Xiong, Y.; Jenekhe, S. A.; Bao, Z.; Xia, Y. *Nano Lett.* **2007**, *7*, 9.
(15) Breeze, A. J.; Salomon, A.; Ginley, D. S.; Gregg, B. A.; Tillmann, H.; Horhold, H. H. *Appl. Phys. Lett.* **2002**, *81*, 3085−7.
(16) Malenfant, P. R. L.; Dimitrakopoulos, C. D.; Gelorme, J. D.; Kosbar, L. L.; Graham, T. O.; Curioni, A.; Andreoni, W. *Appl. Phys. Lett.* **2002**, *80*, 2517–9.
(17) Kim, J. Y.; Bard, A. J. *Chem. Phys. Lett.* **2004**, *383*, 11–15.
(18) Kaneda, Y.; Stawasz, M. E.; Sampson, D. L.; Parkinson, B. A. *Langmuir* **2001**, *17*, 6185–6195.
(19) Rosei, F.; Schunack, M.; Naitoh, Y.; Jiang, P.; Gourdon, A.; Laegsgaard, E.; Stensgaard, I.; Besenbacher, F. *Prog. Surf. Sci.* **2003**, *71*, 95–146.
(20) De Feyter, S.; De Schryver, F. C. *Chem. Soc. Rev.* **2003**, *32*, 139–150.
(21) Perdigão, L. M. A.; Saywell, A.; Fontes, G. N.; Staniec, P. A.; Goretzki, G.; Phillips, A. G.; Champness, N. R.; Beton, P. H. *Chem.—Eur. J.* **2008**, *14*, 7600–7607.

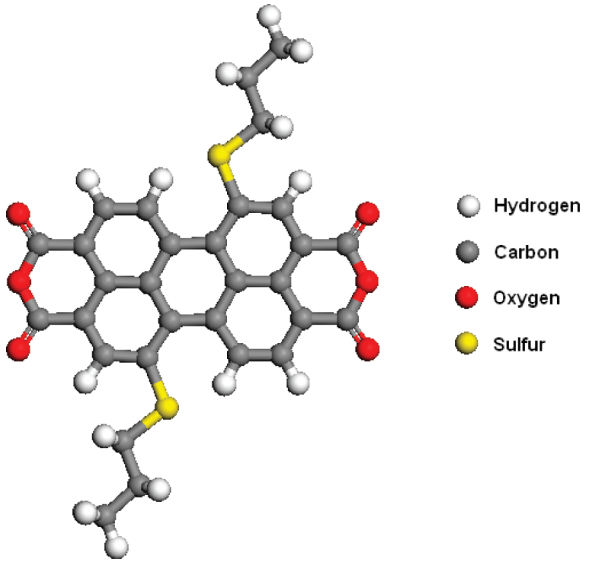


**Figure 1.** Schematic diagram showing the DPT-PTCDA molecule.

checked before solution deposition by imaging the freshly cleaved HOPG substrate. Suitable high-quality tips were left in the microscope to equilibrate overnight before solution deposition. After deposition, the microscope was allowed to thermally stabilize for at least 1 h before the tip was engaged with the sample.

1-Phenyloctane is a nonconductive solvent with minimal evaporation on the time scale of the STM experiments (of the order of 1−2 h). This allowed the STM tip to be immersed in the solution droplet so that scanning took place in situ at the liquid−solid interface. All images were taken at ambient temperature and pressure and acquired by operating the STM in constant current mode with positive tip bias. In order to take account of the orientation of the sample relative to the tip, the gradient plane of images has been subtracted. Images could be acquired only over a narrow range of bias voltages, 0.6−1.4 V, with the most stable operating conditions at ~1 V.

## Results

Images of the DPT-PTCDA layer formed on the HOPG surface are shown in Figure 2. As shown in Figure 2a, the molecules form large, ordered domains with typical widths of ~100 nm in size across greater than 80% of the surface. A periodic contrast variation can be observed across each of the DPT-PTCDA domains. The periodicity of this feature was measured from a number of scans taken in different directions and determined to be $3.0 \pm 0.3$ nm. The contrast modulation is likely due to a commensurability between the adsorbed layer and the underlying HOPG substrate, as noted in the studies of other molecules.[3,4] Figure 2b shows a smaller scan area of one of the domains where an ordered, repeating pattern can be observed. To better understand the images of the DPT-PTCDA layer, we computed the highest occupied molecular orbital (HOMO) of the DPT-PTCDA molecule by performing a density functional theory (DFT) calculation of the orbitals using the DMol$^3$ algorithm.[22,23] An image of the HOMO of DPT-PTCDA produced by this calculation is shown in Figure 3a. The HOMO shown is similar to that presented by Swarbrick et al.[9] for PTCDA but with the addition of two lobes of probability amplitude close to the sulfur atoms in the thioether groups. We propose that the sulfur

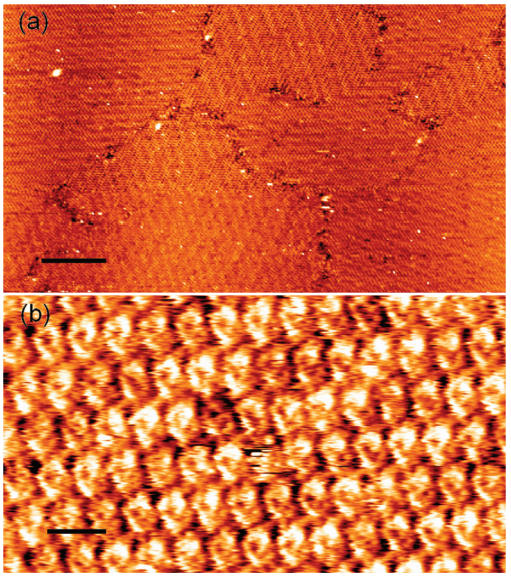


**Figure 2.** (a) An STM image of a DPT-PTCDA monolayer on HOPG demonstrating the size of the domains formed and the periodic contrast modulation. Scale bar 20 nm. (b) A scan of the DPT-PTCDA network showing molecular contrast. Scale bar 2 nm. Scanning parameters for both images: tunnel current, $I$ = 30 pA, tip voltage, $V_{tip}$ = 1 V.

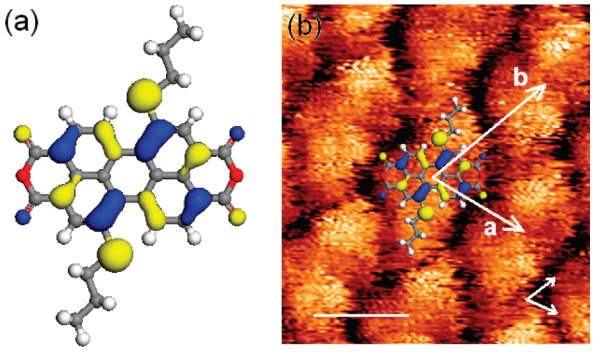


**Figure 3.** (a) Diagram showing the HOMO of the DPT-PTCDA molecule. (b) A diagram showing the HOMO of the DPT-PTCDA molecule overlaid onto an STM image ($I$ = 60 pA, $V_{tip}$ = 0.95 V) to illustrate the orientation of individual molecules in the network. The unit cell dimensions **a** and **b** are shown. Scale bar 1 nm. The orientations of the graphite lattice vectors are shown as black arrows.

atoms give rise to the small areas of higher conductance that appear as bright spots in the STM images. We therefore use these features as a guide for determining the orientation of the molecules in the STM images, as shown in Figure 3b. Note that the intramolecular contrast which is resolved is significantly different to that observed for PTCDA,[18] for which three bright contrast features are resolved.

The displacement vectors between neighboring DPT-PTCDA molecules are identified by vectors **a** and **b** in Figure 3b. Thermal drift was accounted for in the measurement of these distances by obtaining multiple split images, in which areas of both the adsorbed layer and the HOPG substrate were acquired. This was achieved by changing the tunnel voltage halfway through one scan from that used to image the DPT-PTCDA layer to that which reliably images the carbon atoms in the HOPG lattice (see Supporting Information). Such images can be used to compensate for thermal drift in any displacement measurements. The image

(22) Delley, B. *J. Chem. Phys.* **1990**, *92*, 508.
(23) Delley, B. *J. Chem. Phys.* **2000**, *113*, 7756.

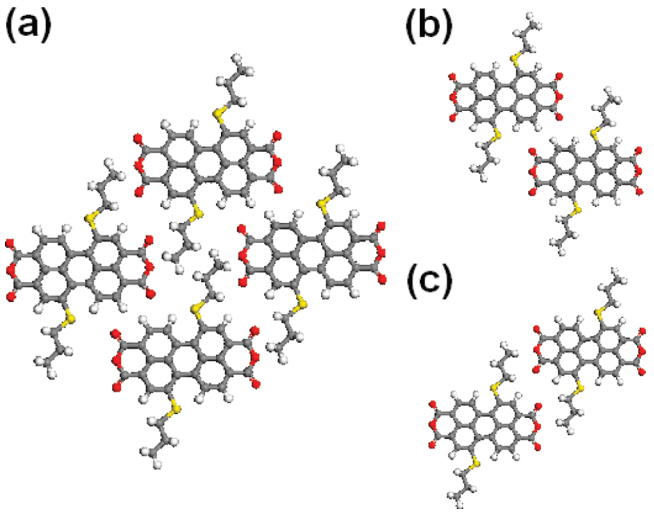


**Figure 4.** (a) Proposed model of DPT-PTCDA on HOPG. (b) Junction along the vector **a**. (c) Junction along the vector **b**.

analysis was performed using the WSxM software.[24] The values for **a** and **b** were averaged from multiple images taken in different scan directions of different areas of the monolayer and were determined to be 1.1 ± 0.1 and 1.3 ± 0.1 nm, respectively, at angles of −16 ± 1° and 58 ± 3° to one of the principal graphite axes.

A model of the DPT-PTCDA network is proposed as shown in Figure 4a. Within this model the molecules are predominantly stabilized by hydrogen bonding between the PTCDA-like cores of adjacent DPT-PTCDA molecules (as in Figure 4b) and hydrogen bonding between the ends of the side chains and the oxygen atoms (as in Figure 4c). It has been well documented that 1-phenyloctane interacts only weakly with the HOPG substrate,[18,25] making the probability of the coadsorption of solvent molecules unlikely, and they are therefore omitted from the model.

In order to gain a better understanding of the stability of the proposed model, DFT calculations were performed using the DMol$^3$ package. Geometry optimizations were performed using the gradient-corrected functional (GGA) proposed by Perdew et al.[26] (PBE), and the double numerical plus polarization (DNP) basis set was used for the orbitals. Simulations did not include any influence of the solvent or the substrate. All carbon, oxygen, and sulfur atoms were constrained such that all molecules in the simulation remained coplanar. This was intended to imitate the constraining effect of the surface on an adsorbed layer and to prevent the simulation from diverging due to the alkane side chains coming out of a planar arrangement. Two geometry optimizations were performed to test the stability of each of the two principal intermolecular junctions, illustrated in Figure 4b,c. These confirmed that both of these hydrogen-bonding configurations are stable with binding energies determined to be −0.272 and −0.196 eV for parts b and c of Figure 4, respectively. The calculated values for **a** and **b** of 1.17 and 1.39 nm, respectively, are in excellent agreement with the experimental results. The calculated O...H separations for the arrangement in Figure 4b is 0.253 nm (between the outer O atom of the anhydride group and the closest H atom bonded to the perylene core). For the arrangement in Figure 4c the minimum O...H separation (between the central O atom of the anhydride group and a hydrogen atom on the alkane chain) is calculated to be 0.258 nm. We note also that our proposed arrangement is near close-packed so that there will be stabilization due to van der Waals interactions in addition to the values calculated using this density functional approach.

## Discussion and Conclusions

Our results show that a large-area coverage of ordered PTCDA derivatives may be deposited from solution. The additional groups that promote solubility also have the effect of suppressing the interaction (between the anhydride group and the perylene core of a nearest-neighbor molecule) which stabilizes the well-known herringbone configuration (see refs 3−9 and 11). This suppression can be understood as a simple steric effect and leads to the proposed configuration in which the perylene cores of the molecules within a given domain are all parallel. The formation of an adsorbed layer of a PTCDA derivative has not been previously reported, and we conclude that this new structure is directly due to the presence of the alkane chain. In addition to van der Waals interactions, the molecular arrangement is stabilized by hydrogen bonding between perylene cores (Figure 4b) and between the additional alkane chain and the anhydride group. The identification of the HOMO allows the S atom positions to be identified and underpins our model of the packing of DPT-PTCDA and its registry with the HOPG substrate.

PTCDA has a number of interesting properties though the poor solubility of the molecule has limited solution-based studies. The new derivative of PTCDA which we report has propyl chains attached via thioether compounds to the sides of the PTCDA molecule, which, importantly, leaves the functionality of the anhydride group intact. This is particularly significant since it has been shown, in vacuum studies, that the anhydride group of PTCDA can act as a donor system in hydrogen-bonded bimolecular junctions.[8] Hydrogen bonding has been widely studied as a route to the introduction and control of molecular order in two-dimensional molecular monolayers of sublimed perylene derivatives.[27−30] More recently, this has been extended to solution deposition,[31] but so far not for a derivative in which the anhydride group is present. We believe that the synthesis and properties of DPT-PTCDA will promote analogue studies of hydrogen bonding in a solution environment, including covalent coupling and, potentially, applications for organic electronic devices.

**Acknowledgment.** This work was supported by the UK Engineering and Physical Sciences Research Council (EPSRC) under Grant EP/D048761/1.

**Supporting Information Available:** An example of a composite image showing the DPT-PTCDA layer and the graphite substrate for drift calibration. This material is available free of charge via the Internet at http://pubs.acs.org.

(24) Horcas, I.; Fernández, R.; Gómez-Rodríguez, J. M.; Colchero, J.; Gómez-Herrero, J.; Baro, A. M. *Rev. Sci. Instrum.* **2007**, *78*, 013705.
(25) De Feyter, S.; De Schryver, F. C. *J. Phys. Chem. B* **2005**, *109*, 4290–4302.
(26) Perdew, J. P.; Burke, K.; Ernzerhof, M. *Phys. Rev. Lett.* **1996**, *77*, 3865.
(27) Theobald, J. A.; Oxtoby, N. S.; Phillips, M. A.; Champness, N. R.; Beton, P. H. *Nature* **2003**, *424*, 1029–1031.
(28) Staniec, P. A.; Perdigão, L. M. A.; Saywell, A.; Champness, N. R.; Beton, P. H. *Chem. Phys. Chem.* **2007**, *8*, 2177–81.
(29) Chen, W.; Li, H.; Huang, H.; Fu, Y. X.; Zhang, H. L.; Ma, J.; Wee, A. T. S. *J. Am. Chem. Soc.* **2008**, *130*, 12285–9.
(30) Stohr, M.; Wahl, M.; Galka, C. H.; Riehm, T.; Jung, T. A.; Gade, L. H. *Angew. Chem., Int. Ed.* **2005**, *44*, 7394–8.
(31) Madueno, R.; Raisanen, M. T.; Silien, C.; Buck, M. *Nature* **2008**, *454*, 618–621.